Data-Driven Robust Predictive Control for Mixed Vehicle Platoons using Noisy Measurement

Jianglin Lan, Dezong Zhao, *Senior Member, IEEE*, and Daxin Tian, *Senior Member, IEEE*

***Abstract*—This paper investigates cooperative adaptive cruise control (CACC) for mixed platoons consisting of both human-driven vehicles (HVs) and automated vehicles (AVs). This research is critical because the penetration rate of AVs in the transportation system will remain unsaturated for a long time. Uncertainties and randomness are prevalent in human driving behaviours and highly affect the platoon safety and stability, which need to be considered in the CACC design. A further challenge is the difficulty to know the exact models of the HVs and the exact powertrain parameters of both AVs and HVs. To address these challenges, this paper proposes a data-driven model predictive control (MPC) that does not need the exact models of HVs or powertrain parameters. The MPC design adopts the technique of data-driven reachability to predict the future trajectory of the mixed platoon within a given horizon based on noisy vehicle measurements. Compared to the classic adaptive cruise control (ACC) and existing data-driven adaptive dynamic programming (ADP), the proposed MPC ensures satisfaction of constraints such as acceleration limit and safe inter-vehicular gap. With this salient feature, the proposed MPC has provably guarantee in establishing a safe and robustly stable mixed platoon despite of the velocity changes of the leading vehicle. The efficacy and advantage of the proposed MPC are verified through comparison with the classic ACC and data-driven ADP methods on both small and large mixed platoons.**

***Index Terms*—Data-driven control, model predictive control, mixed vehicle platoon, reachability.**

I. Introduction

Cooperative adaptive cruise control (CACC), which leverages vehicle-to-vehicle (V2V) wireless communications, ensures a convoy of vehicles travel at the same longitudinal velocity with safe vehicular gaps. Both theoretic and experimental studies have revealed the great potential of CACC in reducing traffic congestion, accidents and fuel consumption [1]–[7]. This has attracted much research interest and many CACC strategies have been developed for effective platooning of pure automated vehicles (AVs) [8], [9]. However, the penetration rate of AVs in the transportation system will remain unsaturated for a long time, resulting in the coexistence of AVs and human-driven vehicles (HVs) on roads [10]. Hence, it is in great need to develop CACC for mixed vehicle platoons consisting of both AVs and HVs. The key difference between the platoon of pure AVs and mixed platoon is that the later involves HVs whose behaviours are not programmable as AVs. Moreover, human driving behaviours have inherent uncertainties and randomness that would cause traffic congestion [11] and oscillation [12]. Therefore, the behaviours of HVs need to be considered in designing the CACC of mixed platoon to ensure platoon safety (i.e., collision-free) and robustness (i.e., formation-maintainable), as demonstrated in the experiments [13]–[15]. However, the state-of-the-art CACC strategies for platooning pure AVs are normally based on the simple and identical mass-point vehicle models and thus cannot be applied to mixed platoons. This raises the demand of developing new CACC strategies for mixed platoons.

Many models have been developed to capture the human driving behaviours in the car-following setting [16], e.g., the intelligent vehicle model, the optimal velocity (OV) model, etc. Compared to other models, the OV model is simple in representation but can characterize qualitatively almost all kinds of traffic behaviours and the transitions between different behaviours [16], [17]. Hence, the OV model has been adopted for analyzing the stability of mixed platoon [18], [19] and developing model-based CACC for AVs within mixed platoons [17], [20]–[24]. Linear quadratic regulators are designed in [20], [21] for controlling an AV to smooth the mixed traffic flow on a ring road. Optimal control is developed in [17] for an AV to lead a number of HVs at a signalized intersection. Tube model predictive control (MPC) is used in [22] to control the AV behind a group of HVs. Robust control is designed in [24] for the AVs in large-scale mixed platoons. However, all the above control designs need to know the parameters of the OV model, which is too restrictive as the HV behaviours are difficult to be modelled exactly [10]. Moreover, both the OV model of HVs and the point-mass model of AVs adopted in the above works do not include the effect of time delays in propulsion, which could affect the platoon stability. Therefore, it is more appealing to develop a CACC for mixed platoons that considers the propulsion time delays and has no need of knowing the HV model (i.e., OV model) parameters.

Adaptive dynamic programming (ADP) [25] has been adopted by [26]–[28] to design data-driven optimal CACC for AVs in the mixed platoon, where the HV model parameters are not required. ADP has been proved powerful to learn optimal stable controllers by utilizing the collected input-state data of the system. However, these works lack a systematic way to guarantee a safe inter-vehicular gap and platoon's robustness against leader velocity changes. Reinforcement learning based

This work was supported in part by the Engineering and Physical Sciences Research Council of the UK under the EPSRC Innovation Fellowship (EP/S001956/1), in part by the UK Royal Society-Newton Advanced Fellowship (NAF\R1\201213), and in part by the National Natural Science Foundation of China (62061130221).

J. Lan is with the Department of Computing, Imperial College London, London SW7 2AZ, UK (email: j.lan@imperial.ac.uk).

D. Zhao is with the James Watt School of Engineering, University of Glasgow, Glasgow G12 8QQ, UK (email: Dezong.Zhao@glasgow.ac.uk).

D. Tian is with the School of Transportation Science and Engineering, Beihang University, Haidian District, Beijing 100191, China (e-mail: dtian@buaa.edu.cn).

CACC for mixed traffic has been developed in [29], where the AVs acceleration commands are generated by a centralized learning model managed on the cloud. The learning model is trained offline using experimental data of mixed traffic to mimic behaviours of the OV model under safety and physical constraints. However, the centralized setting relies on vehicle-to-cloud communications and may cause time delays in applying the acceleration commands. Also, parameters of the learning model are fixed once being trained, which poses challenge in generating optimal CACC for general mixed platoons. All the above data-driven designs have not considered noises in vehicle state measurement and unknown propulsion time delays, which may lead to degraded CACC performance.

To address the above challenges, this paper aims to develop a data-driven MPC for mixed platoons with unknown HV model parameters, unknown propulsion time delays and measurement noise. Due to its capability of real-time optimization and explicit constraint handling, MPC has been widely used for platoons of pure AVs [5]–[7], [9], [30] and also for mixed platoon with known HV models [22]. In principle, the MPC design relies on a known platoon model to predict the future platoon trajectory under the candidate control sequence. The existing model-based MPC designs are inapplicable to this work, because the investigated mixed platoons have unknown models. The proposed design will adopt the technique of system reachability analysis to predict the trajectory of the mixed platoon under specified input and safety constraints. Reachability analysis has been used for autonomous vehicle path planning in [31], but the exact vehicle model is needed. Recently, data-driven reachability analysis has been developed in [32] and used for MPC design for generic discrete-time linear systems in [33]. However, their MPC design requires data sets collected through offline experiments, making it inapplicable for mixed platoon application. In practice a mixed platoon is more likely to be formed on-the-fly and a priori knowledge of it is unavailable. Hence, setting offline simulation experiments for data collection is unrealistic for mixed platoon applications.

The above background motivates this work and the main contributions are summarized as follows:

1) A data-driven robust MPC is proposed to control the ego AVs in the mixed vehicle platoon with unknown HV models. Each vehicle (either AV or HV) is characterized by a third-order dynamic model with an unknown propulsion time delay. The third-order model captures more realistic vehicle dynamics than the second-order point-mass model used in the existing literature on mixed platoons. Moreover, the proposed MPC is applicable for a wide range of mixed platoon formations that contain the one in [26]–[28] as a special case.
2) The proposed MPC explicitly considers input and safety constraints and has provably guarantee in establishing a safe and robustly stable mixed platoon, which is lacking in the data-driven ADP-based designs [26]–[28]. The MPC determines a real-time safe, robust and optimal acceleration command for each ego AV, which has not been realized by either the ADP-based methods [26]–[28] or the reinforcement learning based method [29].
3) The proposed MPC adopts the idea of data-driven reachability and uses vehicle state measurement with unknown noise, which has not been investigated in the literature. The data is collected when the mixed platoon is on-the-fly, rather than collected through offline simulation experiments as in [33]. During data collection, the lead AV generates a small velocity change to excite the platoon dynamics and ego AVs are equipped with the classic adaptive cruise control (ACC) to avoid collisions.

The rest of this paper is organized as follows. Section II describes the mixed platoon and CACC problem, Section III presents the data-driven MPC design, Section IV provides the simulation results, and Section V draws the conclusions.

Notation: The symbol $\mathbb{R}^n$ is the n dimensional Euclidean space. $\otimes$ is the Kronecker product. The superscripts $\top$ and $\dagger$ are transpose and pseudo-inverse, respectively. $|\cdot|$ is the absolute value and $\|x\|_P = x^\top P x$. I_n is a $n \times n$ identity matrix. $\mathbf{1}_n$ is a n dimensional column of ones. $\mathbb{I}_{[a,b]}$ denotes the set of integers from a to b. $\mathbf{0}$ is a zero matrix whose dimensions are known from the context unless it is necessary to be given. s.t. is short for subject to.

II. Mixed Platoon Model and CACC Problem

This paper considers the mixed platoon in Fig. 1, where all the vehicles are equipped with V2V wireless communication devices. The mixed platoon has $N+1$ vehicles, including the lead AV 0, the end AV N, and $N-1$ HVs between them. The role of AV 0 is to ensure controllability of the entire platoon and assist the data collection for designing the proposed data-driven MPC for AV N. AV 0 is assumed to already have a well-tuned controller, e.g., the MPC in [30], to ensure the tracking of reference longitudinal velocity. The focus of this paper is to design the longitudinal acceleration commands of AV N to follow AV 0 by using the motion information from vehicles 0 to $N-1$. The CACC design in this paper is based on Fig. 1, but applicable to more general mixed platoons. This is because a general mixed platoon can be split into multiple sub-platoons with the formation of Fig. 1, which will be demonstrated in the simulation studies.

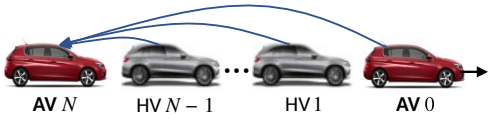

Fig. 1: Formation of the mixed platoon.

The longitudinal dynamics of AVs are characterized by the third-order linear system

$$\begin{aligned} \dot{p}_i &= v_i \\ \dot{v}_i &= a_i \\ \dot{a}_i &= \frac{1}{\tau_i}(u_i - a_i) \end{aligned} \tag{1}$$

where $i = 0, N$. The variables p_i, v_i, a_i, and u_i are the vehicle position, longitudinal velocity, acceleration, and acceleration command, respectively. τ_i is the unknown propulsion time delay.

The acceleration command u_N is to be determined for controlling AV N to track v_0 whilst keeping a safe inter-vehicular gap h^* between itself and HV $N-1$. The platooning error vector of AV N is defined as $x_N = [\Delta h_N \ \Delta v_N \ a_N]^\top$, where $\Delta h_N = h_N - h^*$, $\Delta v_N = v_N - v_0$ and $h_N = p_{N-1} - p_N$. By using (1), the platooning error system of AV N is derived as

$$\dot{x}_N = A_N x_N + B_N u_N + D_N x_{N-1} + E_N a_0 \tag{2}$$

where x_{N-1} is the platooning error vector of HV $N-1$ and

$$A_N = \begin{bmatrix} 0 & -1 & 0 \\ 0 & 0 & 1 \\ 0 & 0 & -\frac{1}{\tau_N} \end{bmatrix}, \ B_N = \begin{bmatrix} 0 \\ 0 \\ \frac{1}{\tau_N} \end{bmatrix},$$
$$D_N = \begin{bmatrix} 0 & 1 & 0 \\ 0 & 0 & 0 \\ 0 & 0 & 0 \end{bmatrix}, \ E_N = \begin{bmatrix} 0 \\ -1 \\ 0 \end{bmatrix}.$$

The car-following behaviour of HV i, $i \in \mathbb{I}_{[1,N-1]}$, is captured by the third-order nonlinear system

$$\begin{aligned} \dot{h}_i &= v_{i-1} - v_i \\ \dot{v}_i &= a_i \\ \dot{a}_i &= \frac{1}{\tau_i}\left[\alpha_i(V(h_i) - v_i) + \beta_i(v_{i-1} - v_i) - a_i\right] \end{aligned} \tag{3}$$

where $h_i = p_{i-1} - p_i$ is the gap between vehicles $i-1$ and i, α_i is the headway gain, and β_i is the relative velocity gain. $V(h_i)$ is the spacing-dependent desired velocity given by [20]:

$$V(h_i) = \begin{cases} 0, & h_i \le h_{\rm s} \\ \frac{v_{\max}}{2}\left[1 - \cos(\pi \frac{h_i - h_{\rm s}}{h_{\rm g} - h_{\rm s}})\right], & h_{\rm s} < h_i < h_{\rm g} \\ v_{\max}, & h_i \ge h_{\rm g} \end{cases} \tag{4}$$

where $h_{\rm s}$ is the smallest gap before the HV intends to stop and $h_{\rm g}$ is the largest gap after which the HV intends to maintain the maximum velocity $v_{\max}$. This paper establishes a stable platoon and thus ensures $h_{\rm s} < h_i < h_{\rm g}$. To build a more realistic mixed platoon model, the HV model (3) includes the acceleration dynamics with unknown propulsion time delay τ_i, which has not been considered in the existing literature on mixed platoons [16]–[24], [26]–[29].

When AV 0 travels at the velocity v_0 ($\le v_{\max}$), the HVs will ultimately reach the equilibrium point (h^*, v^*), where $v^* = v_0$ and h^* satisfies $v^* = V(h^*)$. Define $x_i = [\Delta h_i \ \Delta v_i \ a_i]^\top$, with $\Delta h_i = h_i - h^*$ and $\Delta v_i = v_i - v_0$. The linearized models of the HVs around the equilibrium point are derived as

$$\dot{x}_1 = A_1 x_1, \ \dot{x}_i = A_i x_i + D_i x_{i-1}, \ i \in \mathbb{I}_{[2,N-1]} \tag{5}$$

with

$$A_i = \begin{bmatrix} 0 & -1 & 0 \\ 0 & 0 & 1 \\ \frac{\bar{\alpha}_i}{\tau_i} & \frac{-\bar{\beta}_i}{\tau_i} & \frac{-1}{\tau_i} \end{bmatrix}, \ D_i = \begin{bmatrix} 0 & 1 & 0 \\ 0 & 0 & 0 \\ 0 & \frac{\bar{c}_i}{\tau_i} & 0 \end{bmatrix},$$
$$\bar{\alpha}_i = \alpha_i \hat{\tau}_i, \ \bar{\beta}_i = \alpha_i + \beta_i, \ \bar{c}_i = \beta_i,$$

where $\hat{\tau}_i = V'(h^*)$ is the derivative of $V(h_i)$ with respect to h_i evaluated at h^* [16].

Define the overall platooning error vector as $x = [x_1^\top \ \cdots \ x_N^\top]^\top$ and the control input as $u = u_N$. By using (2) and (5), the overall platooning error system is derived as

$$\dot{x} = A_c x + B_c u + E_c a_0 \tag{6}$$

with the system matrices

$$A_c = \begin{bmatrix} A_1 & & & \\ D_2 & A_2 & & \\ & \ddots & \ddots & \\ & & D_N & A_N \end{bmatrix}, B_c = \begin{bmatrix} B_1 \\ B_2 \\ \vdots \\ B_N \end{bmatrix}, E_c = \begin{bmatrix} E_1 \\ E_2 \\ \vdots \\ E_N \end{bmatrix},$$
$$B_i = \mathbf{0}, \ E_i = \mathbf{0}, \ i \in \mathbb{I}_{[1,N-1]}.$$

The acceleration a_0 of AV 0 is regarded as a disturbance, because it is an external input intending to drift the overall platooning error system (6) away from the equilibrium position. Hence, u will be designed to ensure that the platooning error system is robustly stable against a_0.

Discretizing (6) using the forward Euler method with sampling time t_s to get the control-oriented mixed platoon model

$$\begin{aligned} x(t+1) &= Ax(t) + Bu(t) + Ea_0(t) \\ y(t) &= x(t) + w(t) \end{aligned} \tag{7}$$

where t is the sampling step, $A = I_n + t_s A_c$, $B = t_s B_c$ and $E = t_s E_c$. $w(t)$ is the measurement noise which is unknown but bounded. The dimensions of the vectors $x(t)$, $u(t)$, $a_0(t)$, $y(t)$ and $w(t)$ are $n = 3N$, $m = 1$, $q = 1$, $n = 3N$ and $n = 3N$, respectively.

Although the car-following behaviours of HVs can be captured by the OV model (5), the uncertainty and randomness in human driving make it impossible to identify the exact model parameters α_i and β_i, $i \in \mathbb{I}_{[1,N-1]}$. The propulsion time delays τ_i, $i \in \mathbb{I}_{[1,N]}$, are also unknown. Hence, the system matrices A and B in (7) are unknown and the model-based CACC designs in [17], [18], [20]–[24] are inapplicable. This paper will develop a data-driven MPC to get an optimal $u(t)$ to realize two objectives:

1) Ensure stability of the mixed platoon:

$$Fy(t) - \bar{y}_{\rm r}(t) = 0 \tag{8}$$

where $F = [\mathbf{0}_{3\times(n-3)} \ I_3]$ and $\bar{y}_{\rm r}(t) = [0 \ 0 \ a_0(t)]^\top$.

2) Satisfy input and safety constraints:

$$u(t) \in \mathcal{U}, \ y(t) \in \mathcal{Y} \tag{9}$$

where $\mathcal{U} = \{u \in \mathbb{R} \mid |u| \le u_{\max}\}$ and $\mathcal{Y} = \{y \in \mathbb{R}^n \mid |y| \le y_{\max}\}$, with $y_{\max} = \mathbf{1}_N \otimes \bar{y}$ and $\bar{y} = [\Delta h_{\max} \ \Delta v_{\max} \ u_{\max}]^\top$.

In (9), $u_{\max}$ is the maximum acceleration, $\Delta h_{\max}$ is the maximum allowable inter-vehicular gap error (i.e., deviation from the safe inter-vehicular gap h^*), and $\Delta v_{\max}$ the maximum allowable velocity error (i.e., deviation from the equilibrium velocity v^*). By setting $0 < \Delta h_{\max} < h^*$, satisfying $y(t) \in \mathcal{Y}$ guarantees $0 < p_{i-1} - p_i < 2h^*$ and avoids vehicle collisions.

III. Data-driven robust MPC for mixed platoon

As outlined in Fig. 2, the proposed CACC design consists of three steps:

1) Collect noisy platoon data including the input $u(t)$ and state $y(t)$ (see Section III-B).
2) Construct an over-approximation of the unknown mixed platoon model $[A \ B]$ (see Section III-C). This paper focuses on over-approximating the mixed platoon model,

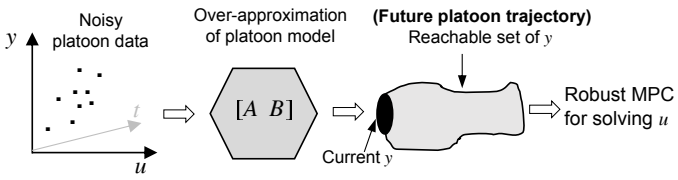

Fig. 2: Flowchart of the proposed CACC design.

because all the possible platoon dynamics under the physical and safety constraints can be captured. Although over-approximation leads to design conservativeness, the over-approximated model is essential for designing MPC to generate a robustly optimal control law $u(t)$ to realize the objectives in (8) and (9).

3) Compute the reachable set of platoon state and design the data-driven robust MPC (see Section III-D).

Before proceeding, the necessary preliminaries of reachability and zonotope are provided in Section III-A.

A. Basics of Reachability and Zonotope

The proposed MPC will be based on the reachable set of the mixed platoon model (7). The reachable set is the union of all possible $y(t)$ within a finite time when starting from the initial state $y(0) \in \mathcal{Y}$ and implementing a set of possible $u(t) \in \mathcal{U}$, in the presence of disturbance $a_0(t)$ and measurement noise $w(t)$. The reachable set is to be computed using the matrix zonotope based set-propagation technique in [31], [32], which can represent the high-dimensional sets compactly and is computationally efficient. This technique is essential for this work, because the state $x(t)$ in the platoon model (7) has the dimension of $n = 3N$, which will be very high as the number of vehicles N increases. The basic knowledge of set representation is recalled from [31], [32] and given below.

Definition 3.1: (Zonotope) Given the center $c_z \in \mathbb{R}^n$ and generator matrix $G_z = [g_z^{(1)} \cdots g_z^{(n_z)}] \in \mathbb{R}^{n \times n_z}$, a zonotope $\mathcal{Z} = \langle c_z, G_z \rangle$ is defined as $\mathcal{Z} = \{x \in \mathbb{R}^n \mid x = c_z + \sum_{i=1}^{n_z} \beta^{(i)} g_z^{(i)},\ |\beta^{(i)}| \le 1\}$.

Definition 3.2: (Matrix zonotope) Given the center matrix $C_m \in \mathbb{R}^{n \times p}$ and generator matrices $G_m = [G_m^{(1)} \cdots G_m^{(n_m)}] \in \mathbb{R}^{n \times n_m p}$, a matrix zonotope $\mathcal{M} = \langle C_m, G_m \rangle$ is defined as $\mathcal{M} = \{X \in \mathbb{R}^{n \times p} \mid X = C_m + \sum_{i=1}^{n_m} \beta^{(i)} G_m^{(i)},\ |\beta^{(i)}| \le 1\}$.

The following operations of zonotope are to be used:

- Linear mapping: $L\mathcal{Z} = \langle Lc_z, LG_z \rangle$.
- Minkowski sum: $\mathcal{Z}_1 + \mathcal{Z}_2 = \langle c_{z1} + c_{z2}, [G_{z1}\ G_{z2}] \rangle$.
- Cartesian product: $\mathcal{Z}_1 \times \mathcal{Z}_2 = \left\langle \begin{bmatrix} c_{z1} \\ c_{z2} \end{bmatrix}, \begin{bmatrix} G_{z1} & 0 \\ 0 & G_{z2} \end{bmatrix} \right\rangle$.
- Interval over-approximation: $\mathcal{Z} = \langle c_z, G_z \rangle$ can be over-approximated by an interval $\mathcal{V} = [\underline{v}, \bar{v}]$, where $\underline{v} = c_z - \sum_{i=1}^{n_z} |g_z^{(i)}|$ and $\bar{v} = c_z + \sum_{i=1}^{n_z} |g_z^{(i)}|$.

In this paper, the reachable set will be computed directly from noisy data with the presence of disturbance $a_0(t)$. The noise $w(t)$ and disturbance $a_0(t)$ are assumed to be unknown but satisfy Assumptions 3.1 and 3.2, respectively.

Assumption 3.1: The measurement noise $w(t)$ is bounded by a zonotope, i.e., $w(t) \in Z_w = \langle c_w, G_w \rangle$ for all $t \ge 0$. The one-step noise propagation $Aw(t)$ is also bounded by a zonotope, i.e., $Aw(t) \in Z_{Aw} = \langle c_{Aw}, G_{Aw} \rangle$ for all $t \ge 0$.

Assumption 3.2: The term $Ea_0(t)$ is bounded by a zonotope, i.e., $Ea_0(t) \in Z_{a_0} = \langle c_{Ea_0}, G_{Ea_0} \rangle$ for all $t \ge 0$.

According to [34], the bound of $Aw(t)$ in Assumption 3.1 can be determined by using the largest singular value of A and the upper bound of $w(t)$. The largest singular value of A could be obtained through experiments by considering model parameter uncertainties of HVs [24]. Assumption 3.1 may be restrictive, but it still remains as an open problem in the field of data-driven control to deal with measurement noise. Since the acceleration $a_0(t)$ of AV 0 is known to satisfy $|a_0(t)| \le u_{\max}$ and the matrix E is known, Assumption 3.2 is always true.

B. Collection of Noisy Mixed Platoon Data

It is seen from (7) that the mixed platoon is influenced by the acceleration a_0 of AV 0. Hence, this paper applies a small time-varying acceleration command $u_0(t)$ to AV 0 to excite the platoon dynamics for data collection. To maintain safety of AV N during data collection, its acceleration command is set as $u(t) = u_{\text{ACC}}(t)$, i.e., the classic ACC controller [35]:

$$u_{\text{ACC}}(t) = \begin{cases} \text{sat}(u_{\text{gap}}(t), u_{\max}), & h_N(t) < d_{\text{safe}}(t) \\ \text{sat}(u_{\text{speed}}(t), u_{\max}), & h_N(t) \ge d_{\text{safe}}(t) \end{cases} \tag{10}$$

where the function "sat()" is defined as $\text{sat}(z, z_{\text{limit}}) := \max(\min(z, z_{\text{limit}}), -z_{\text{limit}})$ such that $|z| \le z_{\text{limit}}$. The gap controller $u_{\text{gap}}(t)$ is used to maintain a safe inter-vehicular gap between HV $N-1$ and AV N:

$$u_{\text{gap}}(t) = k_h(h_N(t) - d_{\text{safe}}(t)) + k_v(v_{N-1}(t) - v_N(t)) \tag{11}$$

where k_h and k_v are constant gains, $d_{\text{safe}}(t)$ is the safe inter-vehicular gap designed as $d_{\text{safe}}(t) = d_{\text{still}} + t_g v_N(t)$, d_{still} is the standstill distance and t_g is the time headway. The speed controller is to control AV N at the specified velocity v_{set} whenever $h_N(t) \ge d_{\text{safe}}(t)$:

$$u_{\text{speed}}(t) = \min(k_s(v_{\text{set}} - v_N(t)), u_{\text{gap}}(t)) \tag{12}$$

where k_s is a constant gain. In this paper, the MATLAB example "Adaptive Cruise Control with Sensor Fusion" is used as the reference to set the values: $k_h = 0.2$, $k_v = 0.4$, $k_s = 0.5$, $d_{\text{still}} = 5$ m, $t_g = 1.5$ s and $v_{\text{set}} = 24.5$ m/s.

The AV N has access to the real-time input $u(t)$ and noisy state measurements $y(t)$ of the system (7). Collect T steps input-state data to obtain the sequences $\{u(t)\}_{t=0}^{T-1}$ and $\{y(t)\}_{t=0}^{T}$. Using them to construct the data set S_{data}:

$$\begin{aligned} S_{\text{data}} &= \{U_-, Y_+, Y_-\},\ U_- = [u(0) \cdots u(T-1)], \\ Y_+ &= [y(1) \cdots y(T)],\ Y_- = [y(0) \cdots y(T-1)]. \end{aligned} \tag{13}$$

The unknown disturbance and noise sequences corresponding to the collected data set S_{data} are denoted as:

$$\begin{aligned} D_- &= [Ea_0(0) \cdots Ea_0(T-1)], \\ W_- &= [w(0) \cdots w(T-1)], \\ W_+ &= [w(1) \cdots w(T)]. \end{aligned} \tag{14}$$

According to Assumptions 3.1 and 3.2, the sequences in (14) satisfy the relations:

$$D_- \subset \mathcal{M}_{a_0},\ W_+ \subset \mathcal{M}_w,\ AW_- \subset \mathcal{M}_{Aw} \tag{15}$$

where the matrix zonotopes $\mathcal{M}_{a_0}$, $\mathcal{M}_w$ and $\mathcal{M}_{Aw}$ are computed from the zonotopes Z_{a_0}, Z_w and Z_{Aw}, respectively.

C. Over-Approximation and Reachable Set of Platoon Model

Due to the existence of measurement noise, there generally exist multiple models $[A\ B]$ that are consistent with the collected data set $S_{\text{data}} = \{U_-, Y_+, Y_-\}$. Under Assumptions 3.1 and 3.2, the zonotopes Z_{a_0}, Z_w and Z_{Aw} that bound $Ea_0(t)$, $w(t)$ and $Aw(t)$ are known. Hence, by collecting enough data such that $[Y_-^\top\ U_-^\top]^\top$ has full rank $n+m$, a matrix zonotope $\mathcal{M}_{AB}$ can be constructed to over-approximate all possible system models (i.e., mixed platoon dynamics) that are consistent with the noisy data, as shown in Lemma 3.1.

Lemma 3.1: Given the data set $S_{\text{data}} = \{U_-, Y_+, Y_-\}$ of the mixed platoon model (7), where $[Y_-^\top\ U_-^\top]^\top$ has full rank $n+m$. Then under Assumptions 3.1 and 3.2, the matrix zonotope

$$\mathcal{M}_{AB} = (Y_+ - \mathcal{M}_{a_0} - \mathcal{M}_w + \mathcal{M}_{Aw}) \begin{bmatrix} Y_- \\ U_- \end{bmatrix}^\dagger \tag{16}$$

contains all possible system models $[A\ B]$ that are consistent with the data and the bounds of disturbance and noise.

Proof: By using (7), the dynamics of $y(t)$ is derived as

$$y(t+1) = Ay(t) + Bu(t) + Ea_0(t) + w(t) - Aw(t+1). \tag{17}$$

Based on (13) and (14), (17) is equivalently written as

$$Y_+ = [A\ B] \begin{bmatrix} Y_- \\ U_- \end{bmatrix} + D_- + W_+ - AW_-. \tag{18}$$

Since the matrix $[Y_-^\top\ U_-^\top]^\top$ has full rank $n+m$, the following equation is derived from (18):

$$[A\ B] = (Y_+ - D_- - W_+ + AW_-) \begin{bmatrix} Y_- \\ U_- \end{bmatrix}^\dagger. \tag{19}$$

By using (15) and (19), the matrix zonotope $\mathcal{M}_{AB}$ in (16) can be used to over-approximate all possible system models $[A\ B]$ that are consistent with the noisy data. ■

Define $\mathcal{R}_t$ as the model-based reachable set of $y(t)$ at time t. Then it is computed based on (17) and given as

$$\mathcal{R}_{t+1} = [A\ B](\mathcal{R}_t \times Z_{u,t}) + Z_{a_0} + Z_w - Z_{Aw} \tag{20}$$

where $\mathcal{R}_0 = \langle y(0), 0\rangle$ and $Z_{u,t} = \langle u(t), 0\rangle$. The data-driven over-approximation of $\mathcal{R}_t$ is provided in Lemma 3.2.

Lemma 3.2: Given the data set $S_{\text{data}} = \{U_-, Y_+, Y_-\}$ of the mixed platoon model (7), where the matrix $[Y_-^\top\ U_-^\top]^\top$ has full rank $n+m$. Then under Assumptions 3.1 and 3.2, the model-based reachable set $\mathcal{R}_t$ is a subset of the data-driven reachable set $\hat{\mathcal{R}}_t$ characterized by

$$\hat{\mathcal{R}}_{t+1} = \mathcal{M}_{AB}(\hat{\mathcal{R}}_t \times Z_{u,t}) + Z_{a_0} + Z_w - Z_{Aw} \tag{21}$$

where $\hat{\mathcal{R}}_0 = \langle y(0), 0\rangle$ and $Z_{u,t} = \langle u(t), 0\rangle$.

Proof: It is easy to see that based on (16) and (20), $\hat{\mathcal{R}}_t$ is governed by (21). Since $[A\ B] \in \mathcal{M}_{AB}$ as shown in Lemma 3.1, it is true that $\mathcal{R}_t \subset \hat{\mathcal{R}}_t$. Therefore, the data-driven representation in (21) provides an over-approximation of the real mixed platoon dynamics in (17). ■

One of the sufficient conditions to the statements in Lemma 3.1 and Lemma 3.2 is collecting "enough data" such that the matrix $[Y_-^\top\ U_-^\top]^\top$ has full rank $n+m$. Physically, this ensures that the dynamic behaviours (acceleration/deceleration) of the mixed platoon are captured by the collected data, so that the unknown parameters α_i and β_i, $i \in \mathbb{I}_{[1,N-1]}$, and τ_i, $i \in \mathbb{I}_{[1,N]}$, in model (7) can be identified from the data [36]. The full rank condition is satisfied if the input $u(t)$ of AV N is persistently exciting of order $n+1$ during data collection [33], [36]. The persistent excitation is realized via designing the input $u(t)$ in [33]. However, this is inapplicable for mixed platoons because $u(t)$ does not influence the behaviours of the HVs ahead of AV N. In this paper, the dynamics of the mixed platoon is excited by applying a small time-varying acceleration command $u_0(t)$ to AV 0, as described in Section III-B. Note that it is also possible to ensure the full rank condition under natural driving (without manually adding extra $u_0(t)$ to AV 0), given that during data collection AV 0 has time-varying velocities that are able to excite fully the dynamics of the mixed platoon. This will be demonstrated through simulations in Section IV-C. Under the natural driving setting, however, it is expected that more time could be taken to collect enough data.

D. Data-Driven Robust MPC Design and Implementation

This section describes the data-driven MPC design based on (21) to realize the platooning objectives in (8) and (9) with robustness against the measurement noise $w(t)$ and leader disturbance $a_0(t)$. As the starting point, the MPC design based on the mixed platoon model (7) is provided to illustrate the basic principle of MPC. At each time step t, the input $u(t)$ is obtained by solving the constrained optimization problem:

$$\min\ J_t(e_y, e_u) \tag{22a}$$

$$\text{s.t. } y(t+k+1|t) = Ay(t+k|t) + Bu(t+k|t) + Ea_0(t+k) + w(t+k) - Aw(t+k),$$

$$\forall w(t+k) \in Z_w,\ \forall Ea_0(t+k) \in Z_{a_0} \tag{22b}$$

$$u(t+k|t) \in \mathcal{U},\ y(t+k+1|t) \in \mathcal{Y} \tag{22c}$$

$$y(t|t) = y(t) \tag{22d}$$

where $J_t(e_y, e_u) = \sum_{k=0}^{N_c-1} \|e_y(t+k+1|t)\|_Q^2 + \|e_u(t+k|t)\|_R^2$ is the cost function, N_c is the prediction horizon, and $e_y(t+k+1|t) = Fy(t+k+1|t) - \bar{y}_{\text{r}}(t)$ and $e_u(t+k|t) = u(t+k|t) - u_{\text{r}}(t)$ are the predicted tracking errors. The input reference $u_{\text{r}}(t) = u_{\text{gap}}(t)$ is the gap controller in (11). $\{u(t+k|t)\}_{k=0}^{N_c-1}$ is the control sequence to be determined, and $y(t)$ is the measured state at time t. The weights $Q \in \mathbb{R}^{3\times 3}$ and $R \in \mathbb{R}^{m\times m}$ are user-specified symmetric positive matrices. The obtained first optimal control input $u^*(t|t)$ is set as $u(t)$ for AV N.

The MPC problem in (22) needs the unknown matrices A and B and thus is not implementable. This paper will reformulate it as a data-driven MPC problem using (21). The key idea is to determine $\{u(t+k|t)\}_{k=0}^{N_c-1}$ at each time step t such that the predicted state sequence $\{y(t+k+1|t)\}_{k=0}^{N_c-1}$ always stay within the computed reachable set and the cost is minimized. The obtained data-driven MPC problem is

$$\min\ J_t(e_y, e_u) \tag{23a}$$

$$\text{s.t. } \hat{\mathcal{R}}(t+k+1|t) = \Big[\mathcal{M}_{AB}(\hat{\mathcal{R}}(t+k|t) \times Z_{u,t}) + Z_{a_0} + Z_w - Z_{Aw}\Big] \cap \mathcal{Y} \tag{23b}$$

$$y(t+k+1|t) \subset \hat{\mathcal{R}}(t+k+1|t) - Z_{a_0} - Z_w + Z_{Aw} \tag{23c}$$

$$u(t+k|t) \in \mathcal{U},\ y(t|t) = y(t) \tag{23d}$$

where $Z_{u,t} = \langle u(t+k|t), 0\rangle$. The constraint in (23b) is the intersection of the reachable set (21) and the state constraint set $\mathcal{Y}$. The combination of (23b) and (23c) is to ensure the predicted state sequence $\{y(t+k+1|t)\}_{k=0}^{N_c-1}$ always stay within the computed reachable set sequence $\{\hat{\mathcal{R}}(t+k+1|t)\}_{k=0}^{N_c-1}$.

The data-driven MPC problem in (23) is solved recursively at each time step to obtain the optimal control input $u(t) = u^*(t|t)$ for AV N. Properties of this data-driven MPC design are described in Theorem 3.1.

Theorem 3.1: Under Assumptions 3.1 and 3.2, if the MPC problem in (23) is feasible at the first time instance t_0, then it is feasible at any time $t \geq t_0$ and the obtained control inputs realize the platooning objectives in (8) and (9), i.e., guaranteeing that the mixed platoon is robustly stable and satisfies the input and safety constraints.

Proof: According to Lemma 3.2, the computed reachable set $\hat{\mathcal{R}}_t$ is the over-approximation of the model-based reachable set $\mathcal{R}_t$, i.e., $\mathcal{R}_t \subset \hat{\mathcal{R}}_t$. The control input sequence is designed to satisfy the constraints in (23b) and (23c). This guarantees that the predicted state is always within the intersection of the over-approximated reachable set and the state constraints regardless of the measurement noise and disturbance. Therefore, feasibility of (23) guarantees robust constraint satisfaction of the over-approximation $\hat{\mathcal{R}}_t$ and of the true reachable set $\mathcal{R}_t$. Feasibility of the problem in (23) also ensures that the predicted state is always enforced within the same constraint set $\mathcal{Y}$. This means that $\mathcal{Y}$ is a constant terminal set of the proposed MPC [30]. Therefore, the MPC problem in (23) is feasible at any time $t \geq t_0$, if it is feasible at the first time instance t_0. ■

According to Theorem 3.1, the velocity deviation $\Delta v_N = v_N - v_0$ satisfies $|\Delta v_N| \leq \Delta v_{\max}$ for any leader acceleration a_0. Hence, it is straightforward to show that the mixed platoon is head-to-tail string stable [37] in the sense of $\mathcal{L}_2$ string stability [26]. For the considered mixed vehicle platoon in Fig. 1, head-to-tail string stability ensures velocity fluctuations to be suppressed from AV 0 to AV N, but allows amplification of velocity fluctuations among the HVs between them. The head-to-tail string stability for a general mixed platoon can be investigated in a similar way by splitting the platoon into multiple sub-platoons [38].

Solving (23) involves computing the matrix zonotopes with intersections and constraints in (23b) and (23c), which is computationally expensive and undesirable for real-time implementation. To overcome this, (23) is reformulated as a more computationally efficient optimization problem:

$$\min \ J_t(e_y, e_u) \tag{24a}$$
$$\text{s.t. } \hat{\mathcal{R}}(t+k+1|t) = \mathcal{M}_{AB}(\hat{\mathcal{R}}(t+k|t) \times Z_{u,t}) + Z_{a_0} + Z_w - Z_{Aw} \tag{24b}$$
$$y(t+k+1|t) + s_u(t+k+1) \leq \mathcal{Y}_u \tag{24c}$$
$$y(t+k+1|t) - s_l(t+k+1) \geq \mathcal{Y}_l \tag{24d}$$
$$y(t+k+1|t) + s_u(t+k+1) \leq \hat{\mathcal{R}}_u(t+k+1|t) \tag{24e}$$
$$y(t+k+1|t) - s_l(t+k+1) \geq \hat{\mathcal{R}}_l(t+k+1|t) \tag{24f}$$
$$s_u(t+k+1) \geq 0, \ s_l(t+k+1) \geq 0 \tag{24g}$$
$$u(t+k|t) \in \mathcal{U}, \ y(t|t) = y(t) \tag{24h}$$

Algorithm 1: Proposed data-driven robust MPC

Require: Input and state constraints $(\mathcal{U}, \mathcal{Y})$, weights (Q, R), and prediction horizon N_c.
for $t \geq 0$ **do**
  while $[Y_-^\top \ U_-^\top]^\top$ *is not full rank* **do**
    Construct $S_{\text{data}} = \{U_-, Y_+, Y_-\}$. ▷ Section III-B
  end
  Compute $\mathcal{M}_{AB}$ using (16). ▷ Section III-C
  Solve (24) for $\{u^*(t+k|t)\}_{k=0}^{N_c-1}$. ▷ Section III-D
  Apply $u(t) = u^*(t|t)$ to AV N.
end

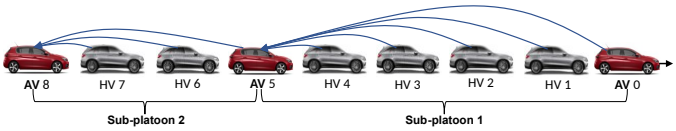

Fig. 3: Simulated mixed platoons: Sub-platoon 1 is used in Sections IV-A and IV-C, while Sub-platoons 1&2 are used in Section IV-B.

where $s_u(t+k+1)$ and $s_l(t+k+1)$ are extra variables introduced to ease the computation. $\mathcal{Y}_u$ and $\mathcal{Y}_l$ are the upper and lower bounds on the individual dimensions of $\mathcal{Y}$, respectively. $\hat{\mathcal{R}}_u(t+k+1|t)$ and $\hat{\mathcal{R}}_l(t+k+1|t)$ are the upper and lower bounds on the individual dimensions of $\hat{\mathcal{R}}(t+k+1|t)$, and they are computed via over-approximating $\hat{\mathcal{R}}(t+k+1|t)$ using an interval, as described in Section III-A.

The only difference between the MPC problems in (23) and (24) is that the constraints in (23b) and (23c) are replaced by (24b) - (24g) with the extra variables $s_u(t+k+1)$ and $s_l(t+k+1)$. Such a replacement improves the computational efficiency whilst retaining the properties proved in Theorem 3.1 and the head-to-tail string stability. The real-time implementation of the proposed CACC is summarized in Algorithm 1.

Remark 3.1: The data collection process in Algorithm 1 is necessary whenever a new mixed platoon forms, e.g., due to lane changes, and cut-ins/outs of vehicles. There may not be time to collect enough data if the platoon formation changes quickly, e.g., at on/off-ramp areas. In such cases, a switch from the data-driven MPC to classic ACC can be made to avoid collisions and ensure safety of the mixed platoon.

IV. Simulation Results

The proposed MPC has been verified in two different mixed platoons: (i) Sub-platoon 1 and (ii) the entire platoon (consisting of Sub-platoons 1&2) in Fig. 3. The Sub-platoons 1&2 have the same formation as Fig. 1 with $N = 5$ and $N = 3$, respectively. The case (ii) is used to demonstrate the applicability of the proposed MPC design for a more general mixed platoon. This has not been investigated in the existing data-driven CACC designs [26]–[28]. Each AV in the platoon is set to not "look beyond" another AV, e.g., AV 8 would not include the V2V signals from those vehicles further ahead than AV 5. This setting is to avoid using unreliable V2V communications between vehicles that are too far apart [39].

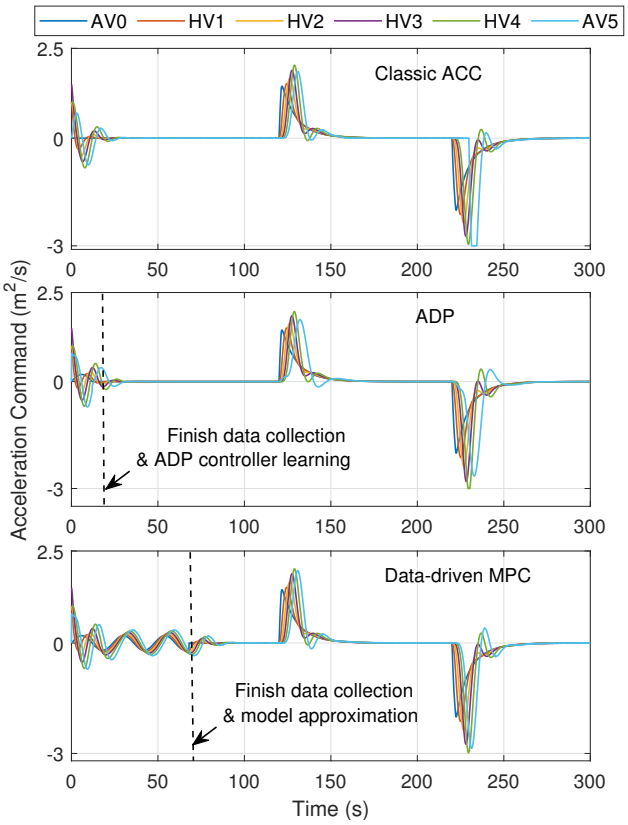

Fig. 4: Vehicle acceleration commands: Sub-platoon 1.

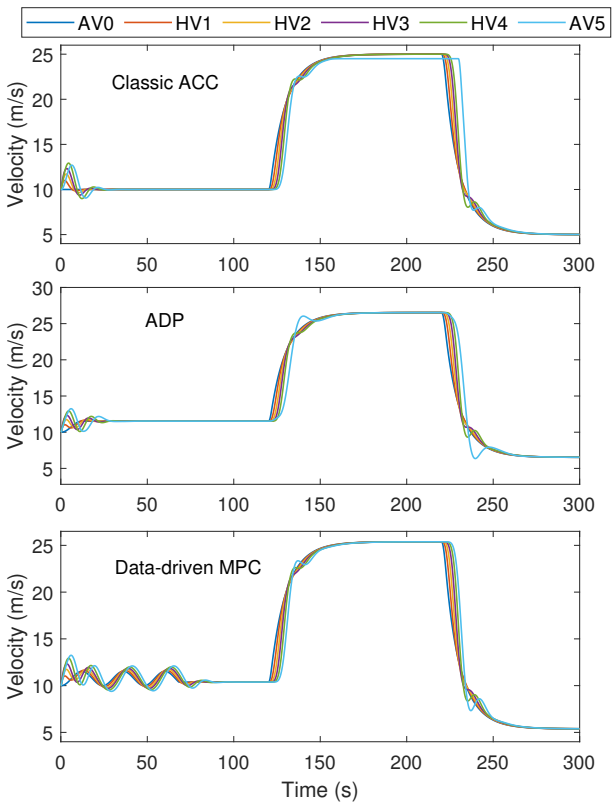

Fig. 5: Vehicle velocities: Sub-platoon 1.

To further demonstrate advantages of the proposed design over the existing ones, three different platooning designs are simulated and compared: *Classic ACC* [35], *ADP* [28], and *Data-driven MPC* proposed in this paper. In the *ADP* design, input-state data are collected for computing the constant gain K_{ADP} to implement the control law $u(t) = -K_{\text{ADP}}x(t)$.

The simulations are conducted in MATLAB by using the toolbox YALMIP [40] with the solver MOSEK [41] for computing the MPC, and the CORA toolbox [42] for computing the zonotopes. To simulate more realistic traffic conditions, the vehicles have the following different model parameters: $\tau_0 = 0.18$ s, $\alpha_1 = 0.2$, $\beta_1 = 0.4$, $\tau_1 = 0.13$ s, $\alpha_2 = 0.2$, $\beta_2 = 0.45$, $\tau_2 = 0.12$ s, $\alpha_3 = 0.3$, $\beta_3 = 0.4$, $\tau_3 = 0.16$ s, $\alpha_4 = 0.2$, $\beta_4 = 0.45$, $\tau_4 = 0.15$ s, $\tau_5 = 0.12$ s, $\alpha_6 = 0.3$, $\beta_6 = 0.5$, $\tau_6 = 0.18$ s, $\alpha_7 = 0.25$, $\beta_7 = 0.4$, $\tau_7 = 0.13$ s, $\tau_8 = 0.14$ s. The propulsion time delays here benchmarked can present many vehicles including power-split plug-in hybrid electric vehicles, such as the 2015 Toyota Prius [43]. The other platoon parameters are: $h_{\text{g}} = 35$ m, $h_{\text{s}} = 5$ m, $v_{\max} = 30$ m/s, $t_s = 0.02$ s, $u_{\max} = 3$ m/s^2, $\Delta h_{\max} = 15$ m, $\Delta v_{\max} = 5$ m/s. The state measurement noise $w(t)$ is a white noise satisfying $|w(t)| \leq 0.01$. The initial vehicle state (p_i, v_i), $i \in \mathbb{I}_{[0,8]}$, are $(160, 10)$, $(140, 10)$, $(120, 10)$, $(100, 10)$, $(80, 10)$, $(60, 10)$, $(40, 10)$, $(20, 10)$ and $(0, 10)$, respectively.

A. Results of Sub-platoon 1

This section presents the comparative simulation results of Sub-platoon 1 in Fig. 3 by applying *Classic ACC*, *ADP*, and *Data-driven MPC* to AV 5. *Classic ACC* is given in (10) with $k_h = 0.2$, $k_v = 0.4$, $k_s = 0.5$, $d_{\text{still}} = 5$ m, $t_g = 1.5$ s and $v_{\text{set}} = 24.5$ m/s, which are the default values in the MATLAB example "Adaptive Cruise Control with Sensor Fusion". *ADP* is designed based on the platoon model (7) and follows Algorithm 1 in [28] with $Q = 10^{-3} \times I_3$ and $R = 1$ but neglecting the driver reaction time. *Data-driven MPC* is designed by running Algorithm 1 in Section III-D with $T = 3400$, $Q = I_3$, $R = 10^{-2}$ and $N_c = 2$. During data collection of *ADP* and *Data-driven MPC*, the excitation signal $u_0(t) = 0.2\sin(\pi t/600)$ m/s^2 is applied to AV 0, and $u_{\text{acc}}(t)$ in (10) is applied to AV 5 with $k_h = 0.2$, $k_v = 0.4$, $k_s = 0.5$, $d_{\text{still}} = 5$ m and $t_g = 1.1$ s. The corresponding gap controller $u_{\text{gap}}(t)$ in (11) is used as the input reference $u_{\text{r}}(t)$ for *Data-driven MPC*.

The vehicle acceleration commands under three designs are shown in Fig. 4. For *ADP* and *Data-driven MPC*, the collected data sequences are required to have the full rank of $n + m$ (which is 16 in this example), where n and m are the dimensions of the platooning model state and the input of AV 5, respectively. However, as seen in Fig. 4, *Data-driven MPC* collects a larger amount of data than *ADP*. This is for constructing a more accurate over-approximation of the platoon model to improve the MPC performance. After finishing data collection, all the three designs have similar acceleration commands that are within the limit $[-u_{\max}, u_{\max}]$, despite of the rapid acceleration and deceleration of AV 0.

As shown in Fig. 5, both *ADP* and *Data-driven MPC* ensure the entire platoon travel at the same velocity. However, for

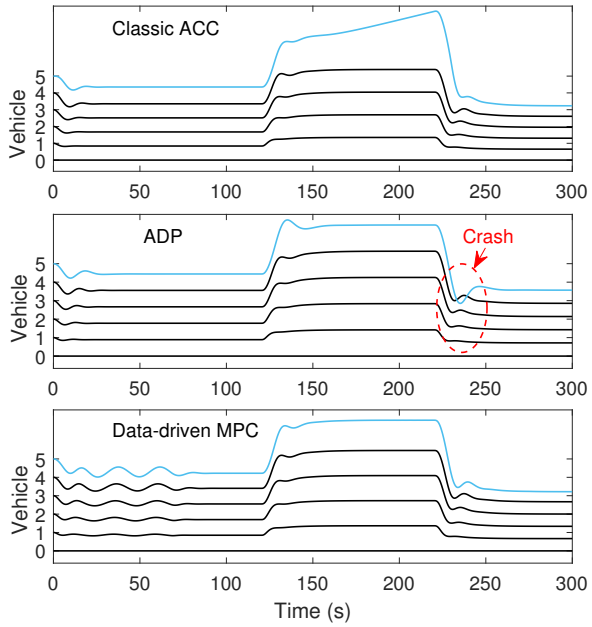

Fig. 6: Relative vehicle positions: Sub-platoon 1.

Classic ACC, AV 5 is set to drive at the constant speed $v_{\text{set}} = 24.5$ m/s whenever $h_N(t) \geq d_{\text{safe}}(t)$. This makes the velocity of AV 5 different from its preceding vehicles at the high speed region during $t \in [150, 240]$ s. Hence, compared to *ADP* and *Data-driven MPC*, *Classic ACC* has larger inter-vehicular gaps between HV 4 & AV 5, as seen in Fig. 6. It is also shown in the middle sub-plot of Fig. 6 that AV 5 crashes into HV 4 under a rapid deceleration of AV 0, due to the lack of considering the safety constraint $y(t) \in \mathcal{Y}$ in *ADP*. The above results demonstrate that *Data-driven MPC* is advantageous in establishing a safe and stable mixed platoon with more compact vehicular gaps, which is beneficial for reducing traffic congestion and fuel consumption.

The computation time to obtain the MPC control input, including computing the data-driven reachable set and the control input sequence, is 0.015 s (on a PC having an Intel(R) i9-10850K CPU 3.60GHz with 32 GB of RAM). This computation time is shorter than the sampling period 0.02 s and does not introduce control input delays.

B. Results of Sub-platoons 1&2

This section presents the comparative simulation results of the entire platoon in Fig. 3 by applying *Classic ACC*, *ADP*, and *Data-driven MPC* to AVs 5&8. *Classic ACC* and *ADP* are designed in the same way as that in Section IV-A. *Data-driven MPC* for AV 5 is also the same as in Section IV-A. *Data-driven MPC* for AV 8 is designed by running Algorithm 1 with $T = 2000$, $Q = I_3$, $R = 10^{-2}$ and $N_c = 3$. It should be emphasized that the data sequences for AVs 5&8 are collected simultaneously, by applying the small time-varying acceleration command $u_0(t)$ to AV 0. During data collection of *ADP* and *Data-driven MPC*, the signals of $u_0(t)$ applied to AV 0, $u_{\text{acc}}(t)$ applied to AVs 5&8, and input reference $u_{\text{r}}(t)$ of AVs 5&8 are identical to those used in Section IV-A.

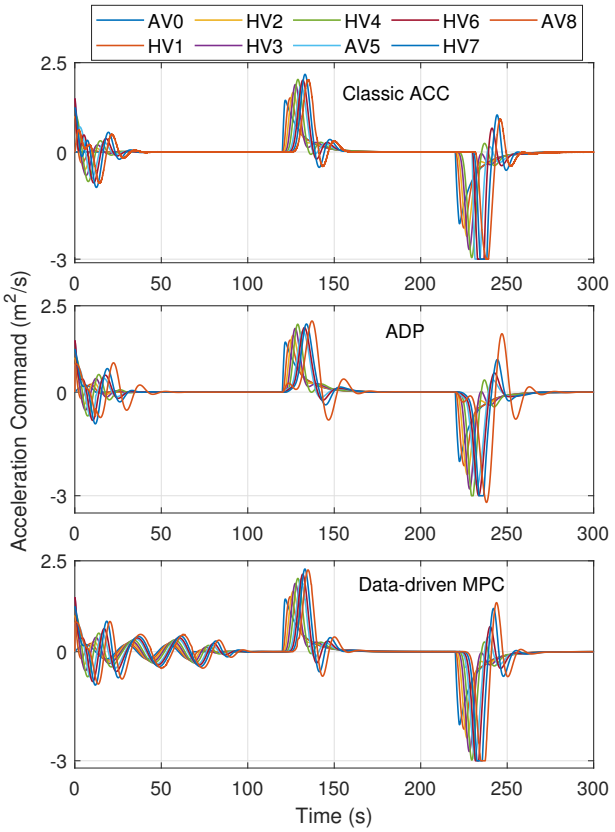

Fig. 7: Vehicle acceleration commands: Sub-platoons 1&2.

It is observed from Fig. 7 that the acceleration commands of all vehicles are within the limit $[-u_{\max}, u_{\max}]$ under *Classic ACC* and *Data-driven MPC*, despite of the rapid acceleration and deceleration of AV 0. However, the acceleration command of AV 8 under *ADP* exceeds the lower limit -3 m/s^2. This is because the input constraint is not considered in *ADP*. As shown in Fig. 8, both *ADP* and *Data-driven MPC* ensure the entire platoon travel at the same velocity. For *Classic ACC*, both AV 5 and AV 8 are set to travel at the constant speed $v_{\text{set}} = 24.5$ m/s when $h_N(t) \geq d_{\text{safe}}(t)$. Since HVs 6&7 follow their immediate predecessors directly, they also travel at the same velocity as AVs 5&8 at steady states. As a result, at the high speed region in $t \in [150, 240]$ s, the entire platoon is split into two sub-platoons that are travelling at different velocities: one sub-platoon consists of AV 0, HV 1, HV 2, HV 3 and HV 4, and the other sub-platoon consists of the rest. Hence, compared to *ADP* and *Data-driven MPC*, *Classic ACC* has larger inter-vehicular gaps between HV 4 & AV 5 and between HV 7 & AV 8 at the high speed region, as seen in Fig. 9. It can also be observed from Fig. 9 that by implementing *ADP*, both AV 5 and AV 8 crash into their front vehicle (HV 4 and HV 7) under a rapid deceleration of AV 0, due to the lack of considering the safety constraint in designing *ADP*.

C. Results of Sub-platoon 1 under Aggressive Leader and Stochastic HV Parameters

This section reports a test of the proposed *Data-driven MPC* on Sub-platoon 1 with an aggressive leader and stochastic

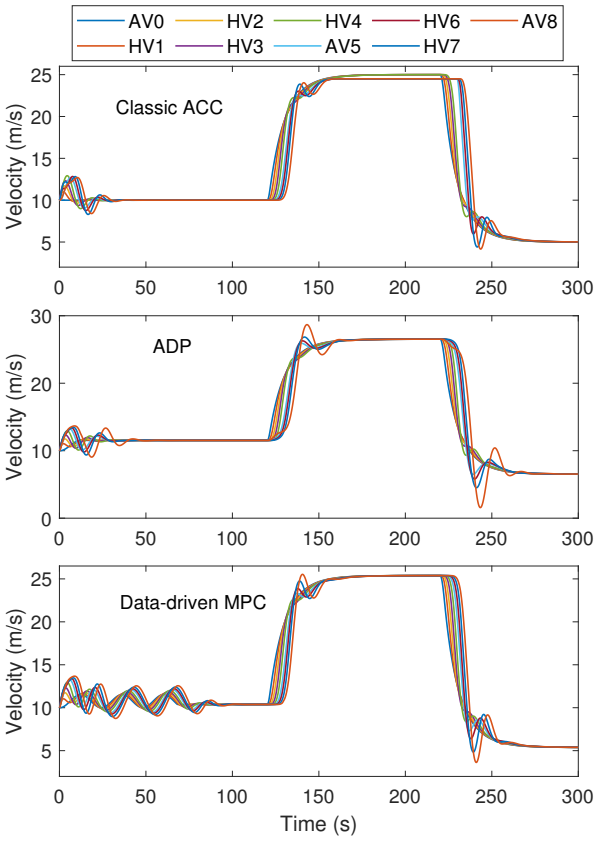

Fig. 8: Vehicle velocities: Sub-platoons 1&2.

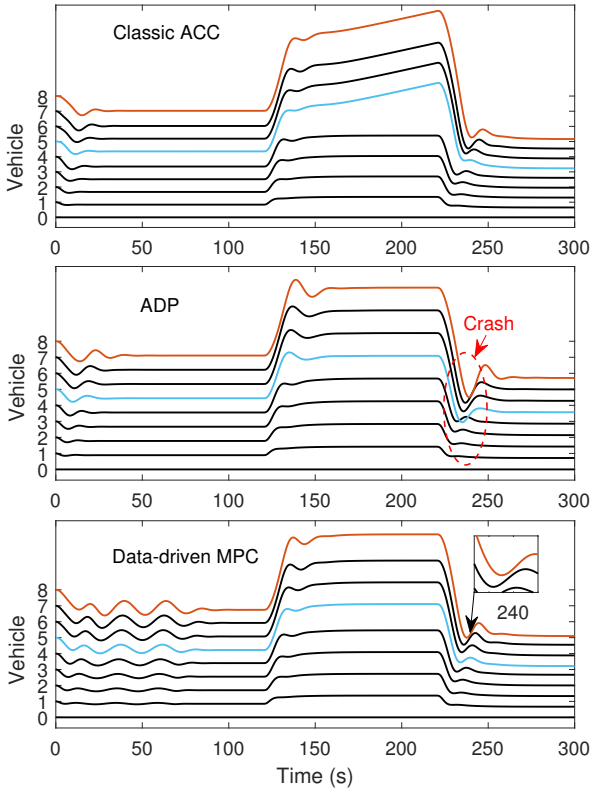

Fig. 9: Relative vehicle positions: Sub-platoons 1&2.

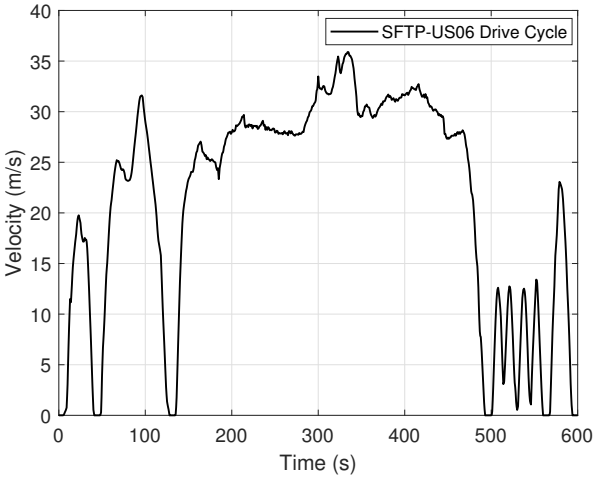

Fig. 10: The SFTP-US06 Drive Cycle.

HVs parameters α_i and β_i, $i \in \mathbb{I}_{[1,4]}$. In the simulation, AV 0 follows the SFTP-US06 Drive Cycle in Fig. 10, which is a representative of aggressive, high speed and/or high acceleration driving behaviour with rapid speed fluctuations. To simulate the uncertainty and randomness in human driving behaviours, the HV model parameters are assumed to have stochastic changes, i.e., $\alpha_1 = 0.2 + \delta(t)$, $\beta_1 = 0.4 + \delta(t)$, $\alpha_2 = 0.2 + \delta(t)$, $\beta_2 = 0.45 + \delta(t)$, $\alpha_3 = 0.3 + \delta(t)$, $\beta_3 = 0.4 + \delta(t)$, $\alpha_4 = 0.2 + \delta(t)$, $\beta_4 = 0.45 + \delta(t)$, where $\delta(t)$ is a white noise satisfying $|\delta(t)| \leq 0.1$. All the other parameters remain the same as Section IV-A, except that $h_{\mathrm{g}} = 50$ m, $v_{\max} = 36$ m/s, $u_{\max} = 4$ m/s^2. Using these h_{g}, $v_{\max}$ and $u_{\max}$ is to ensure the following vehicles have the capability to track the velocity of AV 0 to form a mixed platoon. The initial vehicle positions are the same as in Section IV-A, while the initial velocities are zero, same as AV 0 (see Fig. 10). No excitation signal is applied to AV 0 for data collection. Simulation results show that the *Data-driven MPC* collects enough data within 70 s. As shown in Fig. 11, the acceleration commands of all vehicles are within the limits, and the inter-vehicular distances between each of the two consecutive vehicles are larger than zero. This confirms stability and safety of Sub-platoon 1 under the aggressive leader and HVs with stochastic parameters.

V. Conclusion

This work designs CACC for a mixed platoon consisting of both AVs and HVs. To capture more realistic traffic conditions, the model parameters of HVs are assumed to be unknown and the acceleration dynamics of each vehicle are considered with an unknown propulsion time delay. A data-driven MPC is proposed to obtain the control law of the ego AV in establishing a safe and robustly stable mixed platoon. The MPC design leverages the data-driven reachable sets of the mixed platoon, which are determined based on an over-approximation of the unknown platoon model by collecting noisy vehicle state measurements. The simulation results of both small and large mixed platoons have verified efficacy of the proposed MPC and its advantages over the classic

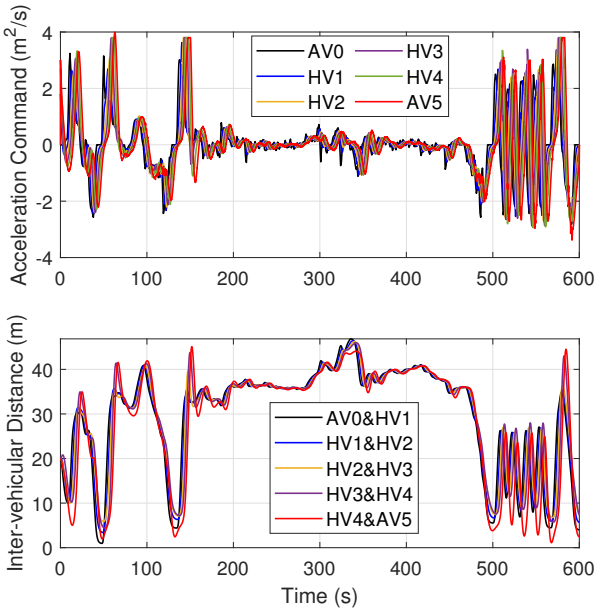

Fig. 11: Vehicle acceleration commands and inter-vehicular distances under the SFTP-US06 Drive Cycle.

ACC and ADP methods in guaranteeing platoon safety and robust stability with smaller vehicular gaps. Although the proposed MPC optimization problem needs to be solved at each sampling step, the simulation results have shown that the computation time is less than the sampling period. Therefore, no time delay will be introduced in implementing the MPC control law. One future work will be extending the proposed design for ecological mixed vehicle platooning. Another will be developing a data-driven MPC for mixed vehicle platoons with consideration of control input delays that are caused by the time delays in actuators, communication and sensors.

REFERENCES

[1] B. Van Arem, C. J. Van Driel, and R. Visser, "The impact of cooperative adaptive cruise control on traffic-flow characteristics," *IEEE Trans. Intell. Transp. Syst.*, vol. 7, no. 4, pp. 429–436, 2006.

[2] C. Chen, L. Liu, T. Qiu, Z. Ren, J. Hu, and F. Ti, "Driver's intention identification and risk evaluation at intersections in the internet of vehicles," *IEEE Internet Things J.*, vol. 5, no. 3, pp. 1575–1587, 2018.

[3] R. Silva and R. Iqbal, "Ethical implications of social internet of vehicles systems," *IEEE Internet Things J.*, vol. 6, no. 1, pp. 517–531, 2018.

[4] H. Guo, J. Liu, Q. Dai, H. Chen, Y. Wang, and W. Zhao, "A distributed adaptive triple-step nonlinear control for a connected automated vehicle platoon with dynamic uncertainty," *IEEE Internet Things J.*, vol. 7, no. 5, pp. 3861–3871, 2020.

[5] C. Zhai, F. Luo, Y. Liu, and Z. Chen, "Ecological cooperative look-ahead control for automated vehicles travelling on freeways with varying slopes," *IEEE Trans. Veh. Technol.*, vol. 68, no. 2, pp. 1208–1221, 2018.

[6] C. Zhai, X. Chen, C. Yan, Y. Liu, and H. Li, "Ecological cooperative adaptive cruise control for a heterogeneous platoon of heavy-duty vehicles with time delays," *IEEE Access*, vol. 8, pp. 146 208–146 219, 2020.

[7] C. Zhai, F. Luo, and Y. Liu, "Cooperative power split optimization for a group of intelligent electric vehicles travelling on a highway with varying slopes," *IEEE Trans. Intell. Transp. Syst.*, doi: 10.1109/TITS.2020.3045264, 2020.

[8] S. E. Li, Y. Zheng, K. Li, Y. Wu, J. K. Hedrick, F. Gao, and H. Zhang, "Dynamical modeling and distributed control of connected and automated vehicles: Challenges and opportunities," *IEEE Intell. Transp. Syst. Mag.*, vol. 9, no. 3, pp. 46–58, 2017.

[9] J. Guanetti, Y. Kim, and F. Borrelli, "Control of connected and automated vehicles: State of the art and future challenges," *Annu. Rev. Control*, vol. 45, pp. 18–40, 2018.

[10] X. Di and R. Shi, "A survey on autonomous vehicle control in the era of mixed-autonomy: From physics-based to AI-guided driving policy learning," *arXiv preprint*, arXiv:2007.05156, 2020.

[11] Y. Sugiyama, M. Fukui, M. Kikuchi, K. Hasebe, A. Nakayama, K. Nishinari, S.-i. Tadaki, and S. Yukawa, "Traffic jams without bottlenecks—experimental evidence for the physical mechanism of the formation of a jam," *New J. Phys.*, vol. 10, no. 3, p. 033001, 2008.

[12] W. B. Qin and G. Orosz, "Experimental validation on connected cruise control with flexible connectivity topologies," *IEEE ASME Trans. Mechatron.*, vol. 24, no. 6, pp. 2791–2802, 2019.

[13] V. Milanés, S. E. Shladover, J. Spring, C. Nowakowski, H. Kawazoe, and M. Nakamura, "Cooperative adaptive cruise control in real traffic situations," *IEEE Trans. Intell. Transp. Syst.*, vol. 15, no. 1, pp. 296–305, 2013.

[14] R. E. Stern, S. Cui, M. L. Delle Monache, R. Bhadani, M. Bunting, M. Churchill, N. Hamilton, H. Pohlmann, F. Wu, B. Piccoli, *et al.*, "Dissipation of stop-and-go waves via control of autonomous vehicles: Field experiments," *Transp. Res. Part C Emerg. Technol.*, vol. 89, pp. 205–221, 2018.

[15] A. Sharma, Z. Zheng, J. Kim, A. Bhaskar, and M. M. Haque, "Assessing traffic disturbance, efficiency, and safety of the mixed traffic flow of connected vehicles and traditional vehicles by considering human factors," *Transp. Res. Part C Emerg. Technol.*, vol. 124, p. 102934, 2021.

[16] G. Orosz, R. E. Wilson, and G. Stépán, "Traffic jams: dynamics and control," *Philos. Trans. A. Math. Phys. Eng. Sci.*, pp. 4455–4479, 2010.

[17] C. Chen, J. Wang, Q. Xu, J. Wang, and K. Li, "Mixed platoon control of automated and human-driven vehicles at a signalized intersection: dynamical analysis and optimal control," *arXiv preprint*, arXiv:2010.16105, 2020.

[18] J. Wang, Y. Zheng, C. Chen, Q. Xu, and K. Li, "Leading cruise control in mixed traffic flow," in *Proc. IEEE Conf. Decis. Control*. IEEE, 2020, pp. 226–232.

[19] R. Drummond and Y. Zheng, "Impact of disturbances on mixed traffic control with autonomous vehicles," in *Proc. IEEE Conf. Decis. Control*. IEEE, 2020, pp. 220–225.

[20] Y. Zheng, J. Wang, and K. Li, "Smoothing traffic flow via control of autonomous vehicles," *IEEE Internet Things J.*, vol. 7, no. 5, pp. 3882–3896, 2020.

[21] V. Giammarino, S. Baldi, P. Frasca, and M. L. Delle Monache, "Traffic flow on a ring with a single autonomous vehicle: An interconnected stability perspective," *IEEE Trans. Intell. Transp. Syst.*, vol. 22, no. 8, pp. 4998–5008, 2021.

[22] S. Feng, Z. Song, Z. Li, Y. Zhang, and L. Li, "Robust platoon control in mixed traffic flow based on tube model predictive control," *arXiv preprint*, arXiv:1910.07477, 2019.

[23] L. Wanga and B. K. Hornb, "On the stability analysis of mixed traffic with vehicles under car-following and bilateral control," *IEEE Trans, Autom. Control*, vol. 65, no. 7, pp. 3076–3083, 2020.

[24] D. Hajdu, I. G. Jin, T. Insperger, and G. Orosz, "Robust design of connected cruise control among human-driven vehicles," *IEEE Trans. Intell. Transp. Syst.*, vol. 21, no. 2, pp. 749–761, 2019.

[25] F. L. Lewis, D. Vrabie, and K. G. Vamvoudakis, "Reinforcement learning and feedback control: Using natural decision methods to design optimal adaptive controllers," *IEEE Control Syst.*, vol. 32, no. 6, pp. 76–105, 2012.

[26] W. Gao, Z.-P. Jiang, and K. Ozbay, "Data-driven adaptive optimal control of connected vehicles," *IEEE Trans. Intell. Transp. Syst.*, vol. 18, no. 5, pp. 1122–1133, 2016.

[27] M. Huang, W. Gao, and Z.-P. Jiang, "Connected cruise control with delayed feedback and disturbance: An adaptive dynamic programming approach," *Int. J. Adapt. Control Signal Process.*, vol. 33, no. 2, pp. 356–370, 2019.

[28] M. Huang, Z. P. Jiang, and K. Ozbay, "Learning-based adaptive optimal control for connected vehicles in mixed traffic: Robustness to driver reaction time," *IEEE Trans. Cybern.*, doi:10.1109/TCYB.2020.3029077, 2020.

[29] T. Chu and U. Kalabić, "Model-based deep reinforcement learning for CACC in mixed-autonomy vehicle platoon," in *Proc. IEEE Conf. Decis. Control*. IEEE, 2019, pp. 4079–4084.

[30] J. Lan and D. Zhao, "Min-max model predictive vehicle platooning with communication delay," *IEEE Trans. Veh. Technol.*, vol. 69, no. 11, pp. 12 570–12 584, 2020.

[31] M. Althoff, "Reachability analysis and its application to the safety assessment of autonomous cars," Ph.D. dissertation, Technische Universität München, 2010.
[32] A. Alanwar, A. Koch, F. Allgöwer, and K. H. Johansson, "Data-driven reachability analysis using matrix zonotopes," *arXiv preprint, arXiv:2011.08472*, 2020.
[33] A. Alanwar, Y. Stürz, and K. H. Johansson, "Robust data-driven predictive control using reachability analysis," *arXiv preprint, arXiv:2103.14110*, 2021.
[34] C. De Persis and P. Tesi, "Formulas for data-driven control: Stabilization, optimality, and robustness," *IEEE Trans. Autom. Control*, vol. 65, no. 3, pp. 909–924, 2019.
[35] S. E. Shladover, D. Su, and X.-Y. Lu, "Impacts of cooperative adaptive cruise control on freeway traffic flow," *Transp. Res. Rec.*, vol. 2324, no. 1, pp. 63–70, 2012.
[36] J. C. Willems, P. Rapisarda, I. Markovsky, and B. L. De Moor, "A note on persistency of excitation," *Syst. Control. Lett.*, vol. 54, no. 4, pp. 325–329, 2005.
[37] I. G. Jin and G. Orosz, "Optimal control of connected vehicle systems with communication delay and driver reaction time," *IEEE Trans. Intell. Transp. Syst.*, vol. 18, no. 8, pp. 2056–2070, 2016.
[38] M. R. Hidayatullah and J.-C. Juang, "String stability criterion for mixed vehicular platoons," in *Proc. Int. Autom. Control Conf.* IEEE, 2020, pp. 1–6.
[39] D. Jia, H. Chen, Z. Zheng, D. Watling, R. Connors, J. Gao, and Y. Li, "An enhanced predictive cruise control system design with data-driven traffic prediction," *IEEE Trans. Intell. Transp. Syst.*, doi: 10.1109/TITS.2021.3076494, 2021.
[40] J. Löfberg, "YALMIP: A toolbox for modeling and optimization in MATLAB," in *Proc. CACSD*, vol. 3, 2004.
[41] Mosek ApS, "The MOSEK optimization software." [Online]. Available: https://www.mosek.com
[42] M. Althoff, "An introduction to CORA 2015," in *Proc. ARCH*, 2015.
[43] Y. Lin, J. McPhee, and N. L. Azad, "Comparison of deep reinforcement learning and model predictive control for adaptive cruise control," *IEEE Trans. Intell. Transp. Syst.*, vol. 6, no. 2, pp. 221–231, 2020.

Jianglin Lan received the Ph.D. degree from University of Hull in 2017. He has held several Research Associate positions, currently at Imperial College London, and previously at University of Glasgow, Loughborough University, and University of Sheffield. His research interests include machine learning, optimization and control for autonomous systems.

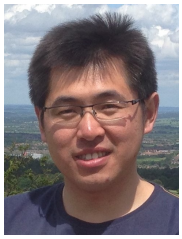

Dezong Zhao (M'12–SM'17) received the B.Eng. and M.S. degrees from Shandong University in 2003 and 2006, respectively, and the Ph.D. degree from Tsinghua University in 2010. He is a Senior Lecturer at University of Glasgow, and was a Lecturer at Loughborough University. He has been an EPSRC Innovation Fellow since 2018 and a Royal Society-Newton Advanced Fellow since 2020. His research interests include connected and autonomous vehicles, machine learning and control engineering.

Daxin Tian (M'13–SM'16) is currently a Professor in the School of Transportation Science and Engineering, Beihang University, China. He is an IEEE Senior Member, IEEE Intelligent Transportation Systems Society Member, and IEEE Vehicular Technology Society Member, etc. His current research interests include mobile computing, intelligent transportation systems, vehicular ad hoc networks, and swarm intelligent.